machines

MDPI

Article

Mechanical Looseness Diagnosis Using Wavelet Packet Energy Analysis and Supervised Feature Relevance Evaluation

Marta Zamorano [1,*], María Jesús Gómez [2,3] and Cristina Castejon [2,3]

[1] Higher Polytechnic School, Universidad Francisco de Vitoria, Crta. Pozuelo-Majadahonda km 1,800, 28223 Pozuelo de Alarcón, Madrid, Spain
[2] Mechanical Engineering Department, Universidad Carlos III de Madrid, Avda. Universidad 30, 28911 Leganés, Madrid, Spain; mjggarci@ing.uc3m.es (M.J.G.); castejon@ing.uc3m.es (C.C.)
[3] Pedro Juan de Lastanosa Research Institute, Universidad Carlos III de Madrid, Avda. Universidad 30, 28911 Leganés, Madrid, Spain
* Correspondence: marta.zamorano@ufv.es

Abstract

Mechanical looseness is one of the most common faults affecting rotating machinery and may lead to severe degradation or catastrophic failure if not detected at early stages. This paper presents a vibration-based methodology for looseness diagnosis in rotating shafts using Wavelet Packet Transform (WPT) energy analysis and supervised feature relevance evaluation. Experiments were conducted on a rotating machinery test bench under healthy and defective conditions with an artificially introduced diametral clearance of 0.5 mm. Vibration signals acquired at different rotational speeds were processed through WPT to extract packet energy features from the time-frequency domain. Neighborhood Component Analysis (NCA) was employed to evaluate the discriminative capability of the extracted features and to investigate the distribution of looseness-related information across the WPT packets. The results revealed that mechanical looseness generates characteristic energy redistribution patterns concentrated within specific frequency regions and that rotational speed significantly influences the localization and separability of the fault-related vibration components. The influence of different mother wavelets was additionally analyzed, showing clear operating-condition-dependent differences in the discriminative relevance of the extracted WPT energy features.

Keywords: mechanical looseness; rotating machinery; Wavelet Packet Transform; mother wavelet selection; Neighborhood Component Analysis; vibration analysis; fault diagnosis; condition monitoring

Academic Editors: Cai Yi and Qiuyang Zhou

Received: 28 May 2026
Revised: 1 July 2026
Accepted: 10 July 2026
Published: 12 July 2026

1. Introduction

Rotating machinery is widely used in industrial sectors, including manufacturing, transportation, energy production, and automated production systems. Failures in rotating components can generate severe economic losses, operational downtime, and safety hazards. Consequently, the development of reliable condition monitoring systems has become a critical research topic in modern industrial engineering [1–4].

Traditional maintenance strategies were based on corrective interventions performed after failures occurred. Although this approach minimizes initial maintenance costs, unexpected failures may cause severe disruptions in industrial production lines. Preventive maintenance strategies were introduced to mitigate these risks by performing periodic inspections and component replacements regardless of the actual machine condition [2,5].

Recent advances in Industry 4.0 technologies have enabled the development of predictive maintenance frameworks in which sensors, data acquisition systems, and intelligent algorithms continuously monitor the operational state of industrial machines. In predictive maintenance, faults are detected during operation before catastrophic failures occur, enabling optimized maintenance planning and improved system reliability [3,6,7].

Among the faults affecting rotating machinery, mechanical looseness represents one of the most frequent and potentially damaging conditions. Looseness typically originates from assembly errors, mechanical wear, insufficient tightening of mechanical components, or dimensional tolerances between interacting elements such as shafts, couplings, bearings, and housings [8]. When mechanical looseness develops, intermittent contact between components produces impacts, nonlinear vibration behavior, and energy transfer across a wide frequency spectrum. Early-stage detection is particularly challenging because looseness may generate weak and non-stationary vibration components masked by other dynamic phenomena [9,10].

Vibration analysis has long been recognized as one of the most effective diagnostic tools for rotating machinery. Changes in vibration signals often reveal the presence of mechanical defects before they become visually detectable. Frequency domain techniques such as Fast Fourier Transform (FFT) remain widely used for fault detection; however, these methods may present limitations when analyzing non-stationary signals [11,12].

To overcome these limitations, time–frequency signal processing methods have been extensively investigated in recent years. Wavelet-based approaches have demonstrated strong capabilities for analyzing non-stationary signals and extracting fault-related features from rotating machinery vibrations [1,13]. Recent studies have further highlighted the importance of advanced time–frequency representations for improving diagnostic robustness under varying operating conditions [14,15].

The selection of an appropriate mother wavelet remains one of the main challenges in wavelet-based fault diagnosis, as the chosen wavelet directly affects the quality of the time–frequency representation and the separability of fault-related features [16–18]. In many previous studies [19–21], mother wavelet selection has commonly been performed using empirical methodologies based on energy distributions, statistical indicators, or application-specific criteria [22]. Although these methodologies may provide satisfactory diagnostic performance, they are often based on empirical criteria that do not guarantee an objective or interpretable assessment of the discriminative capability of the extracted features. As a result, the systematic evaluation of mother wavelets under varying operating conditions remains an open challenge in rotating machinery diagnostics [18,23].

The Wavelet Packet Transform (WPT) extends classical wavelet analysis by recursively decomposing both approximation and detail components of the signal, providing improved frequency resolution. Previous studies have demonstrated that WPT energy features can effectively characterize vibration signals generated by mechanical faults in rotating machinery [20,24]. Recent studies have explored the use of machine learning techniques not only for fault classification but also for feature relevance analysis and representation optimization in vibration-based diagnostics. Supervised feature relevance analysis can provide quantitative information regarding the discriminative capability of extracted features, enabling more objective evaluation of signal processing strategies under different operating conditions [25–28].

The present study proposes a methodology for mechanical looseness diagnosis in rotating shafts based on WPT energy analysis and supervised feature relevance evaluation. Neighborhood Component Analysis (NCA) was employed to quantitatively evaluate the discriminative capability of the extracted WPT energy features under different rotational speeds. The study further investigates how rotational speed influences the distribution of vibration energy across the WPT packets and analyzes the influence of different mother wavelets on the obtained time–frequency representations.

The main contributions of this work are: (i) supervised relevance analysis of WPT energy features for mechanical looseness diagnosis, (ii) an interpretability-oriented assessment of vibration energy redistribution under varying operating conditions, and (iii) analysis of the influence of rotational speed and mother wavelets on WPT-based fault characterization.

2. Materials and Methods

The proposed methodology combines experimental vibration acquisition, Wavelet Packet Transform (WPT)-based feature extraction, and supervised feature relevance evaluation using Neighborhood Component Analysis (NCA) in order to assess the capability of different mother wavelets to characterize mechanical looseness in a controlled rotating shaft test rig.

2.1. Experimental Test Bench and Fault Implementation

The experimental setup, shown in Figure 1, consisted of a scaled rotating shaft mounted on a laboratory test rig, namely a Machinery Fault Simulator by SpectraQuest® (Richmond, VA, USA) [29]. The test bench included an electric motor, a mechanical coupling, a rotating shaft, two bearing supports, and an accelerometer mounted on the bearing housing closest to the motor. The shaft was supported by two Rexnord (Milwaukee, WI, USA) ER10K bearings and driven by the motor through the mechanical coupling.

Figure 1. Experimental test bench used for vibration acquisition, showing the motor, mechanical coupling, rotating shaft, bearing supports, and accelerometer mounted on the bearing housing closest to the motor.

The shaft geometry was based on a 1:8 scaled railway axle. However, the test rig was not intended to reproduce the complete dynamic behavior of a full-scale in-service railway axle. In the present work, it was used as a controlled and repeatable rotating shaft system for evaluating looseness-related vibration signatures. Therefore, the results should be interpreted as laboratory validation of the proposed diagnostic methodology, while further tests under realistic loading and full-scale operating conditions would be required before extrapolating the results to actual railway axle applications.

The healthy shaft was made of aluminium and had a diameter of 20.77 mm in the central body and 15.00 mm in the journal sections, where the shaft was supported by the bearings and connected to the motor coupling. The main shaft dimensions relevant to the experimental setup are summarized in Figure 2.

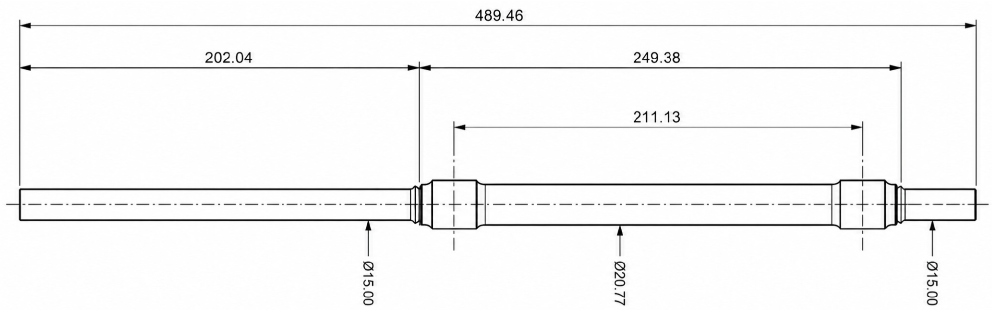

Figure 2. Simplified geometry of the scaled shaft used in the experimental test bench, showing the main longitudinal dimensions, the central body diameter, and the journal sections where the looseness condition was introduced.

Mechanical looseness was reproduced by manufacturing and testing a second shaft with the same material and overall geometry as the healthy shaft, but with a reduced diameter only in the journal sections. In the defective shaft, the journal diameter was reduced from 15.00 mm to 14.50 mm, while the central body diameter remained unchanged. As a result, a controlled diametral clearance of 0.5 mm was generated between the shaft and the motor coupling, as well as between the shaft and the bearings.

Therefore, the looseness condition was introduced through a repeatable geometric modification of the shaft rather than by randomly loosening screws or altering the bearing supports. The presence of clearance at both the motor coupling and the bearings was a direct consequence of the reduced-diameter journal sections. This configuration represents a controlled shaft-interface looseness condition affecting both torque transmission and shaft support.

The imposed clearance should be interpreted as a laboratory fault severity selected to generate measurable intermittent contact and nonlinear dynamic behavior, rather than as an incipient looseness condition. No external load or braking resistance was applied during the tests; therefore, the experiments were conducted under controlled laboratory operating conditions.

2.2. Signal Acquisition and Preprocessing

Vibration signals were acquired using a Brüel & Kjær 4383 uniaxial piezoelectric accelerometer (HBK-Hottinger Brüel & Kjær, Nærum, Denmark) mounted on the bearing housing closest to the motor. Data acquisition was performed after the shaft reached steady-state rotational speed, in order to avoid transient effects associated with startup or speed stabilization. The sampling frequency was 6000 Hz. Each independent vibration signal consisted of 16,384 samples, corresponding to an acquisition duration of approximately 2.73 s. This signal length was selected to ensure sufficient temporal information for WPT-based time–frequency analysis while preserving computational efficiency and compatibility with dyadic wavelet decomposition schemes.

For each rotational speed condition (20 Hz, 40 Hz, and 60 Hz), 100 independent vibration signals were acquired under healthy operating conditions and 100 independent vibration signals under mechanical looseness conditions. This resulted in balanced datasets for supervised feature relevance evaluation, with 200 signals per rotational speed and 600 signals in total. These operating conditions were selected to investigate the influence of rotational speed on vibration energy distribution and on the suitability of different mother wavelets for looseness characterization.

The number of independent signals was selected to provide a representative set of repeated measurements for each class while maintaining a balanced dataset for NCA-based supervised feature relevance evaluation. The use of the same number of healthy and looseness signals avoids class imbalance effects and enables direct comparison of WPT packet-energy distributions under the different rotational speeds.

Prior to feature extraction, the acquired signals were pre-processed through detrending and amplitude normalization in order to reduce offset components, minimize signal variability, and improve feature consistency during the WPT analysis.

2.3. Wavelet Packet Transform

The Wavelet Packet Transform (WPT) was selected due to its capability to recursively decompose both approximation and detail coefficients, providing enhanced frequency resolution over the entire frequency spectrum [30]. WPT is based on the Discrete Wavelet Transform (DWT), in which the analyzed signal is decomposed through low-pass and high-pass filtering operations.

In the conventional DWT, a signal containing (N) samples is decomposed into approximation coefficients (A), obtained through low-pass filtering, and detail coefficients (D), obtained through high-pass filtering (Figure 3).

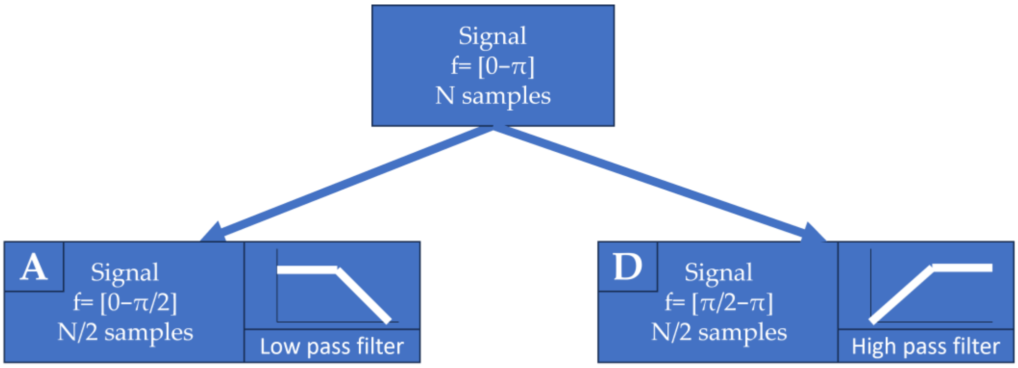

Figure 3. DWT decomposes the signal into approximation information (A) and detail information (D).

This decomposition enables simultaneous time–frequency representation of non-stationary signals. The WPT recursively decomposes both approximation and detail coefficients (up to a selected decomposition level k), leading to improved frequency resolution across the full spectrum. Consequently, WPT provides a more detailed representation of transient vibration energy distributions associated with looseness-induced dynamic behavior.

In Figure 4, which shows a WPT decomposition tree, W (*k*, *j*), represents the set of wavelet packet coefficients associated with the packet located at decomposition level (*k*) and packet position (*j*), as defined in Equation (1).

$$\mathrm{W}(k,j) = \{w_1(k,j),\ldots,w_N(k,j)\} = \{w_i(k,j)\} \quad (1)$$

For each vibration signal, a level-3 (*k*) WPT decomposition was performed, resulting in eight frequency packets. For a decomposition level k and sampling frequency f_s, the WPT decomposition divides the frequency range from 0 to $f_s/2$ into 2^k packets. Therefore, for the level-3 decomposition used in this study and a sampling frequency of 6000 Hz, the eight WPT packets had a nominal bandwidth of 375 Hz.

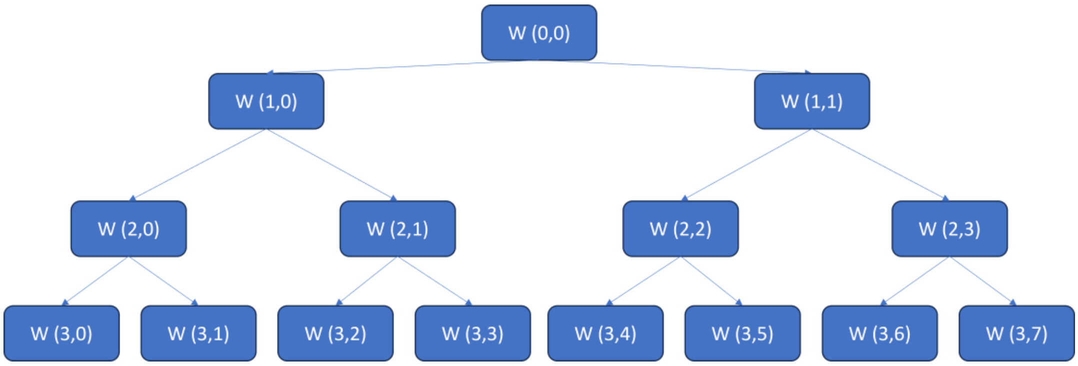

Figure 4. WPT decomposition for a level-3 decomposition.

A level-3 decomposition was selected as a compromise between frequency resolution, computational simplicity, and interpretability of the WPT energy distribution. The objective of the proposed methodology was not to achieve highly localized spectral decomposition, but rather to evaluate the capability of different mother wavelets to characterize the global redistribution of vibration energy associated with mechanical looseness under varying rotational speeds. Consequently, level-3 decomposition was considered appropriate for objective comparative wavelet evaluation.

Since each terminal WPT packet represents a specific frequency band, the energy within each frequency band was computed from the corresponding wavelet packet coefficients. For the packet located at decomposition level (k) and packet position (j), the packet-energy feature was calculated as:

$$E(k,j) = \sum_{i=1}^{N} \{w_i(k,j)\}^2, \tag{2}$$

where $E(k,j)$ represents the energy of the frequency band associated with packet $\mathrm{W}(k,j)$, $w_i(k,j)$ denotes the i-th wavelet packet coefficient of that packet, and N is the number of coefficients in the packet. Consequently, each vibration signal was represented by an 8-dimensional feature vector composed of the packet energies.

Additional decomposition levels may provide improved spectral localization of fault-related information and were therefore further investigated after the comparative mother wavelet evaluation.

It should be noted that the WPT packet numbering does not necessarily correspond to ascending frequency order. Therefore, the frequency ranges associated with each packet were identified according to the corresponding decomposition bands used in the present analysis.

2.4. Mother Wavelet Evaluation

One of the key parameters affecting the performance of the Wavelet Packet Transform (WPT) is the selected mother wavelet. Different wavelet families exhibit distinct time–frequency localization capabilities, regularity properties, symmetry characteristics, and compact support lengths, which may significantly influence the resulting WPT energy distributions and the separability of fault-related vibration features.

The present study focused on three widely used discrete wavelet families commonly employed in vibration-based fault diagnosis: Daubechies (db), Symlets (sym), and Coiflets (coif). These wavelet families were selected due to their suitability for discrete WPT implementations, their compact support properties, and their well-established capability for representing transient and non-stationary vibration signals in rotating machinery applications [19–21].

The evaluated mother wavelets included db2–db10, sym2–sym10, and coif1–coif5. The Haar wavelet (db1) was excluded from the analysis due to its discontinuous shape and limited smoothness, which may reduce its capability to accurately represent transient vibration phenomena associated with looseness-induced impacts.

Although the selected wavelet families share several mathematical properties, including compact support and suitability for discrete signal decomposition, differences in symmetry, regularity, filter length, and vanishing moments may significantly influence the resulting WPT energy distributions. Consequently, a comparative evaluation was required to identify the most suitable mother wavelet for each operating condition.

For each evaluated mother wavelet, WPT decomposition was performed for all vibration signals, packet energies were extracted, and a feature matrix of size (200×8) was generated. Each row of the matrix corresponded to one vibration signal, while each column represented the energy associated with one WPT packet. Before feature relevance analysis, all features were standardized using z-score normalization.

2.5. Feature Relevance Analysis Using Neighborhood Component Analysis

To quantitatively evaluate the discriminative capability of the extracted WPT energy features, Neighborhood Component Analysis (NCA) was employed [31]. NCA is a supervised feature weighting and dimensionality reduction technique that assigns relevance weights according to the contribution of each feature to class separability. The algorithm optimizes feature weights by maximizing the separation between samples belonging to different classes while preserving neighborhood relationships among samples of the same class. Consequently, features contributing more strongly to the discrimination between healthy and looseness conditions receive higher relevance weights.

Given the feature matrix $X \in \mathbb{R}^{200\times 8}$ and the corresponding class labels: $Y \in \{0,1\}^{200}$, where 0 represents healthy condition and 1 represents mechanical looseness condition, NCA assigns a relevance weight to each WPT packet according to its contribution to the separability between both classes. The overall discriminative capability of each mother wavelet was quantified through the cumulative NCA relevance score:

$$S = \sum_{i=1}^{8} w_i \tag{3}$$

where w_i denotes the relevance weight associated with the (i)-th WPT packet, and S represents the cumulative discriminative score of the analyzed mother wavelet. Higher cumulative scores indicate that the corresponding mother wavelet produces WPT energy features with greater capability to distinguish between healthy and looseness conditions. Consequently, the proposed methodology enables objective comparative evaluation of different mother wavelets based on supervised feature relevance analysis rather than empirical or visually interpreted criteria.

2.6. Comparative Analysis

Finally, the cumulative NCA scores obtained for all evaluated mother wavelets were compared in order to identify the most suitable wavelet configuration for each operating condition.

In addition to the global relevance score, the distribution of individual NCA weights across the WPT packets was analyzed to identify the frequency regions most sensitive to looseness-induced vibration behavior. This comparative analysis enabled the evaluation of how different mother wavelets represented fault-related energy redistribution within the time–frequency domain under varying rotational speeds.

Consequently, the proposed methodology enables:

- Objective mother wavelet evaluation based on supervised feature relevance analysis;
- Quantitative comparison of WPT-based time–frequency representations;
- Identification of informative WPT frequency regions for looseness characterization;
- Assessment of the influence of rotational speed on vibration energy redistribution.

To improve the clarity and reproducibility of the proposed methodology, the complete WPT–NCA workflow is summarized in Figure 5.

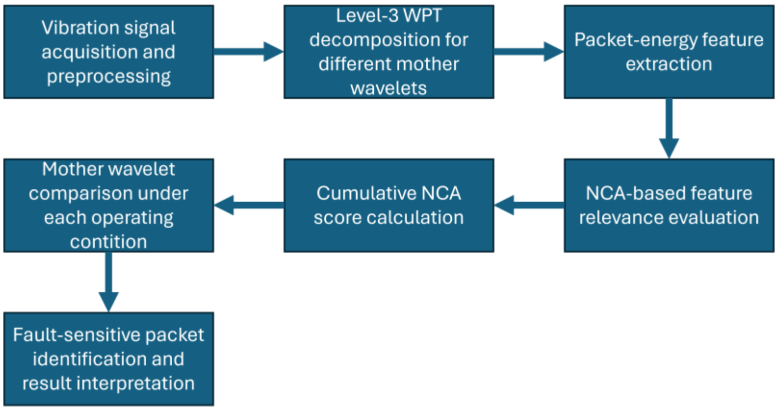

Figure 5. Flowchart of the proposed WPT–NCA methodology for mechanical looseness diagnosis.

3. Results and Discussion

3.1. Time-Domain Vibration Analysis

Figure 6 presents representative vibration signals acquired under healthy and looseness conditions at 60 Hz rotational speed.

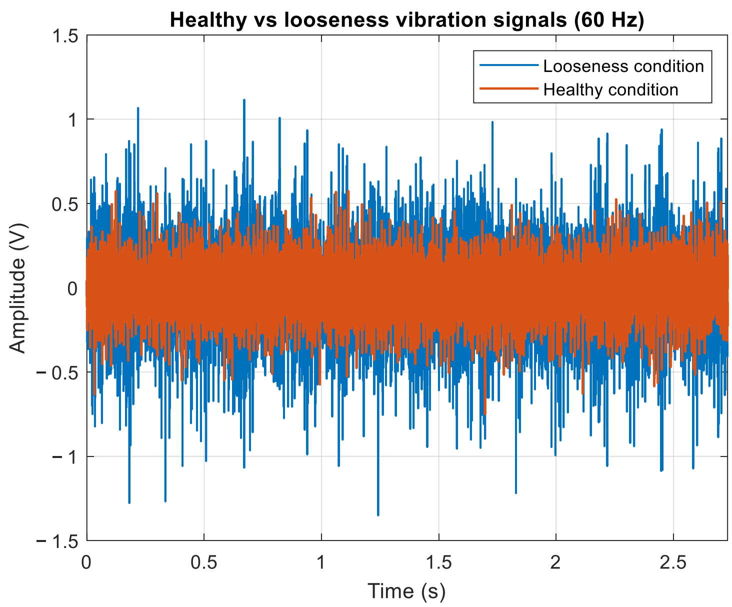

Figure 6. Time-domain vibration signals acquired under healthy and looseness conditions (60 Hz).

The looseness condition exhibits larger amplitude fluctuations and more impulsive transient behavior compared with the healthy condition. These effects are associated with intermittent mechanical contacts and nonlinear dynamic interactions generated by looseness within the rotating assembly.

The observed non-stationary behavior justifies the use of time–frequency analysis techniques such as WPT for fault characterization.

3.2. Comparative Mother Wavelet Evaluation

Figure 7 presents the cumulative NCA relevance scores obtained for all evaluated mother wavelets under the three analyzed rotational speed conditions.

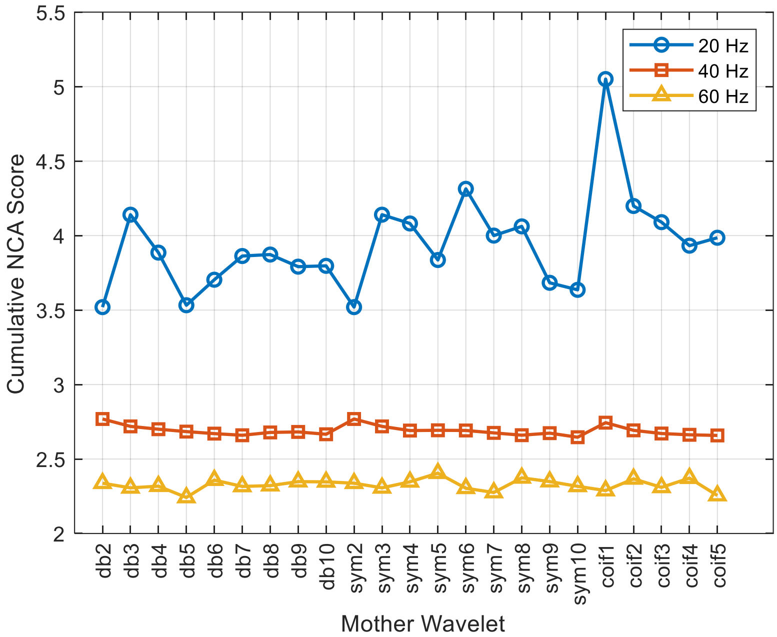

Figure 7. Cumulative NCA relevance scores for all evaluated mother wavelets.

The cumulative NCA relevance score was used as a relative supervised metric to compare the discriminative capability of the WPT packet-energy features obtained with different mother wavelets. For a given rotational speed, all mother wavelets were evaluated using the same dataset, the same WPT decomposition level, the same number of packet-energy features, and the same NCA configuration. Therefore, differences in the cumulative NCA score reflect changes in the overall supervised relevance of the feature set generated by each mother wavelet. This score should be interpreted as a comparative relevance indicator within the same operating condition, rather than as an absolute measure of fault severity or vibration energy.

A clear variation in the cumulative scores can be observed among the evaluated wavelet families, indicating that the selected mother wavelet significantly influences the discriminative capability of the extracted WPT energy features.

The results additionally reveal a strong influence of rotational speed on the distribution of feature relevance. The highest cumulative NCA scores were generally obtained under the 20 Hz operating condition, whereas lower cumulative scores were observed at 40 Hz and 60 Hz. It should be noted that these cumulative NCA scores are primarily used here for the comparative evaluation of mother wavelets within each operating condition, rather than as a direct measure of the absolute fault severity or vibration energy separation between different rotational speeds. Therefore, the lower cumulative scores obtained at higher speeds do not necessarily imply a weaker physical manifestation of looseness, but rather indicate that the discriminative information is distributed and weighted differently within the WPT feature space.

Under the 20 Hz condition, the highest discriminative capability was obtained using the coif1 mother wavelet, which produced a substantially larger cumulative NCA score than the remaining evaluated wavelets. At 40 Hz, the highest cumulative NCA relevance score was obtained using sym2, whereas at 60 Hz the best-performing mother wavelet was sym5. These results demonstrate that the optimal mother wavelet depends on the operating condition and cannot be considered independent of rotational speed. Consequently, the proposed supervised relevance analysis methodology enables objective operating-condition-dependent wavelet selection instead of relying on empirical or visually interpreted criteria.

3.3. Wavelet Packet Relevance Analysis

To investigate how the discriminative capability was distributed within the WPT decomposition, the individual NCA relevance weights associated with each packet were analyzed through heatmap representations.

Figure 8 presents the packet relevance distributions obtained under the 20 Hz operating condition for all evaluated mother wavelets. A clear concentration of relevance can be observed in packets P3 (1125–1500 Hz) and P7 (1500–1875 Hz), which consistently exhibit the highest NCA weights across most evaluated wavelets. This behavior indicates that looseness-related vibration information is primarily concentrated within specific WPT frequency regions rather than uniformly distributed across the spectrum.

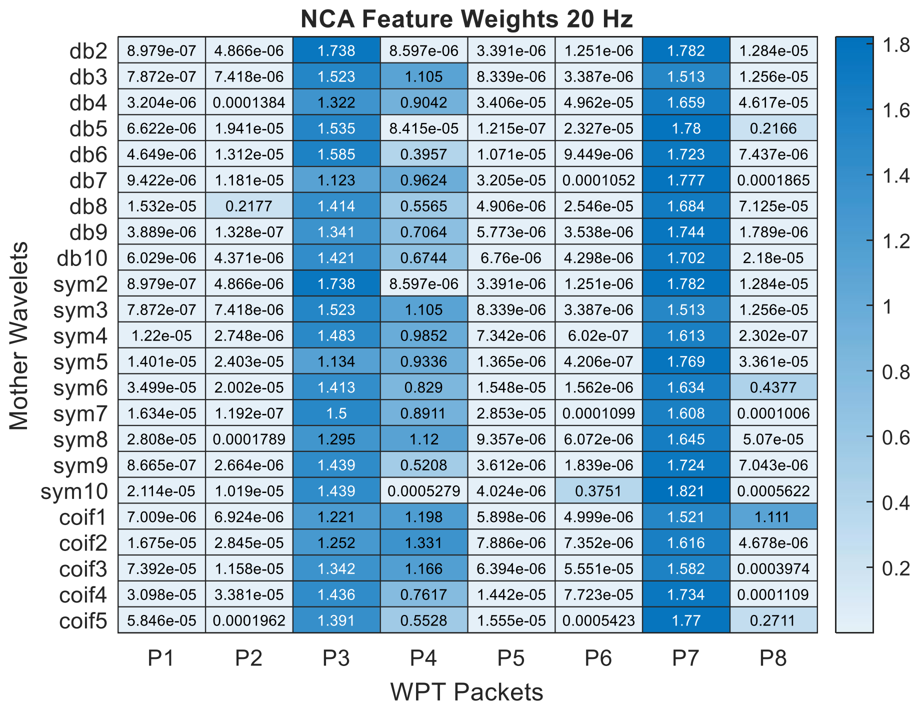

Figure 8. NCA feature weights at 20 Hz.

At 40 Hz rotational speed (Figure 9), the relevance distribution exhibits a substantial redistribution toward lower-frequency packets. Compared with the 20 Hz condition, where dominant relevance was concentrated in packets P3 and P7, the 40 Hz condition reveals stronger contributions from packets P1 (0–375 Hz) and P3 (1125–1500 Hz). These results suggest that the frequency regions most sensitive to mechanical looseness vary significantly with rotational speed.

Under the 60 Hz operating condition (Figure 10), the relevance distribution becomes strongly concentrated in packet P6 (2250–2625 Hz) for nearly all evaluated mother wavelets. Compared with the lower-speed conditions, the obtained results reveal a progressive evolution toward more localized and spectrally structured fault-related representations as rotational speed increases.

The obtained heatmap distributions demonstrate that rotational speed significantly influences both the WPT energy redistribution and the localization of diagnostically informative frequency regions.

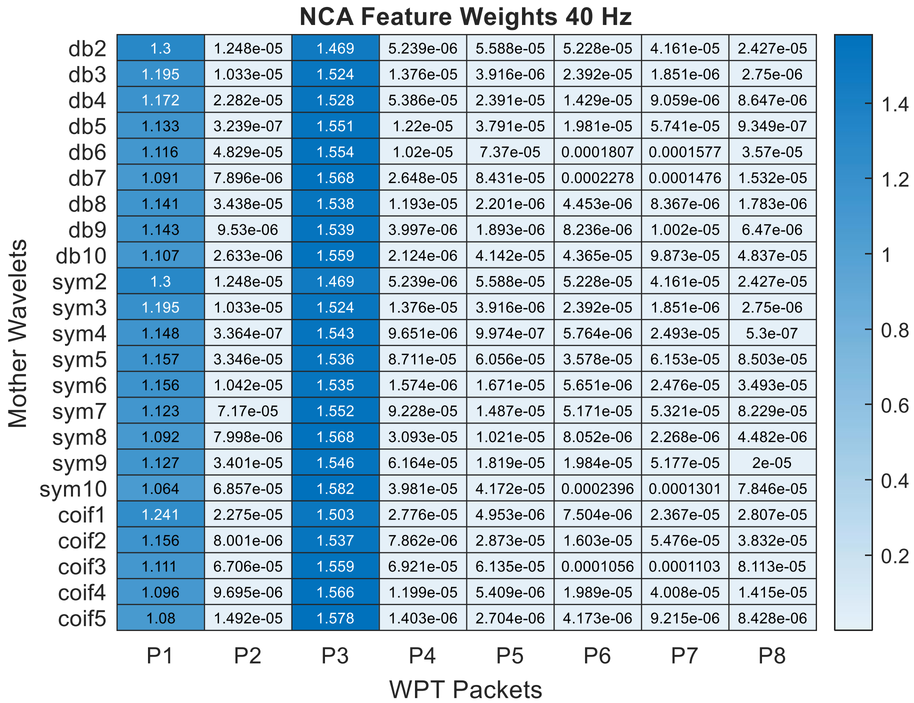

Figure 9. NCA feature weights at 40 Hz.

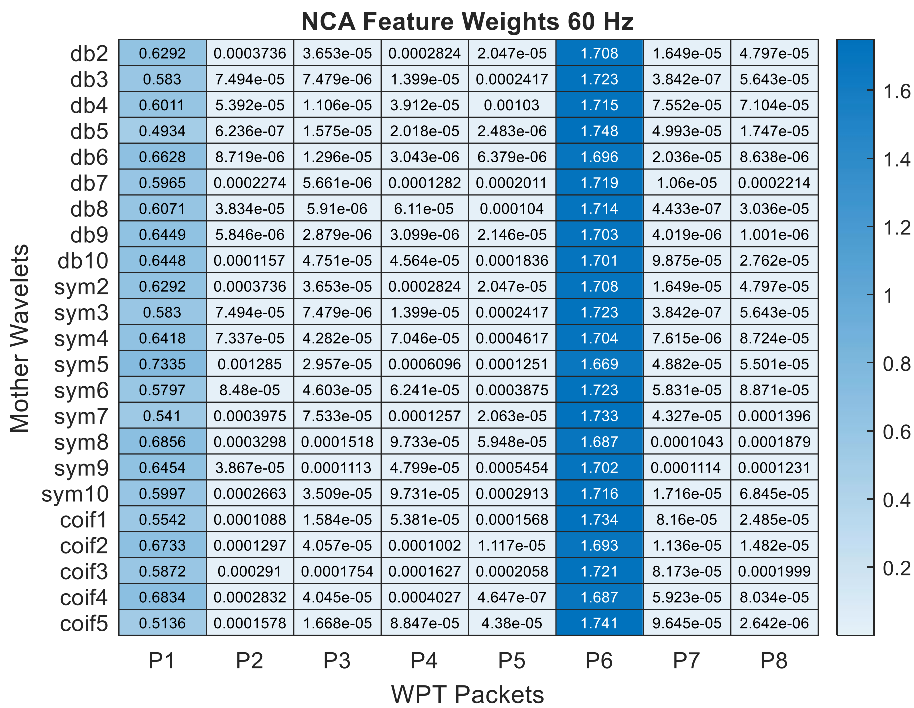

Figure 10. NCA feature weights at 60 Hz.

3.4. Statistical Validation Through Boxplot Analysis

To further investigate the physical interpretability of the NCA relevance distributions, boxplot representations of the WPT packet energies were analyzed for healthy and looseness conditions under different rotational speeds.

The boxplots enable visualization of the packet energy distributions, the overlap between operating conditions, and the sensitivity of individual WPT frequency regions to looseness-induced vibration changes. Therefore, the boxplot analysis was used as a descriptive tool to support the physical interpretation of the WPT energy redistribution, rather than as a formal statistical significance test.

These boxplot results complement the NCA relevance analysis by providing a direct visualization of the energy distributions associated with healthy and looseness conditions. While the cumulative NCA score was used to compare the discriminative relevance of WPT features among different mother wavelets within each rotational speed, the boxplots illustrate the absolute energy variation and class overlap for each packet. Consequently, both analyses should be interpreted as complementary: NCA identifies the most informative WPT packets for supervised discrimination, whereas the boxplots provide physical insight into how the vibration energy is redistributed under mechanical looseness.

At 20 Hz rotational speed (Figure 11), the boxplot analysis shows visible differences between healthy and looseness conditions in several WPT packets. Packets P3 and P7 exhibited strong class separation and were also identified as highly relevant by the NCA analysis. However, packets P4 and P8 also showed noticeable differences between both conditions, although their relative supervised relevance was lower than that of the most dominant packets. This indicates that visual separation in individual boxplots and NCA-based feature relevance provide complementary information. While the boxplots illustrate the univariate distribution of packet energies, NCA evaluates the contribution of each packet to supervised class separability within the complete WPT feature space.

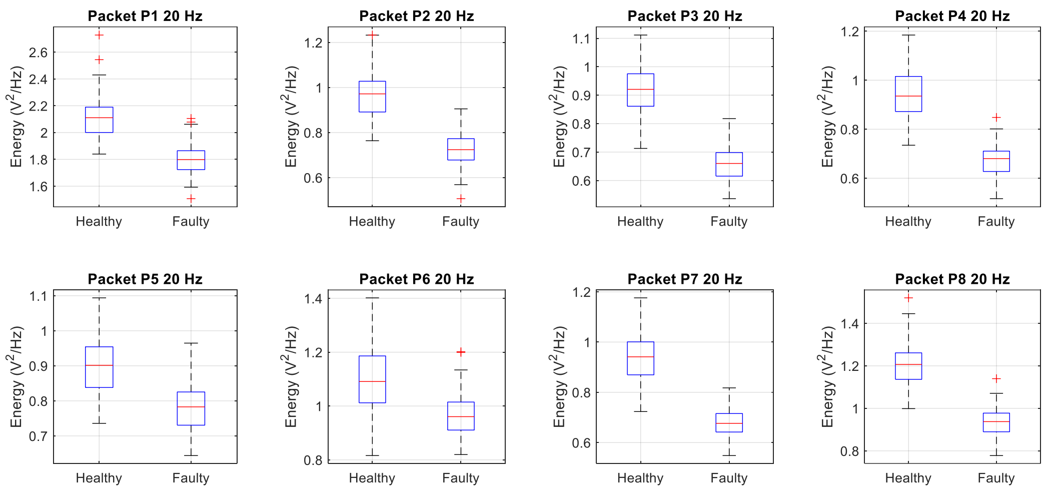

Figure 11. Boxplot representation of WPT packet energy distributions under healthy and looseness conditions at 20 Hz rotational speed. The boxes represent the interquartile range, the central line indicates the median value, and the dashed whiskers indicate the range of non-outlier data points according to the default boxplot convention used in the analysis.

At 40 Hz (Figure 12), the vibration behavior became considerably more complex. Several WPT packets exhibited increased energy under faulty conditions, whereas others showed energy reduction. This behavior suggests that mechanical looseness does not simply amplify vibration amplitudes, but rather redistributes vibration energy across multiple frequency regions through nonlinear dynamic interactions and intermittent contact phenomena.

At 60 Hz rotational speed (Figure 13), the energy differences between healthy and looseness conditions became more pronounced for most WPT packets. Most packets exhibited substantial energy increases under faulty conditions with minimal overlap between class distributions. These results suggest that increasing rotational speed intensifies the vibration energy variations associated with mechanical looseness, although the supervised NCA relevance remains concentrated in specific WPT packets, as previously observed in Figure 10.

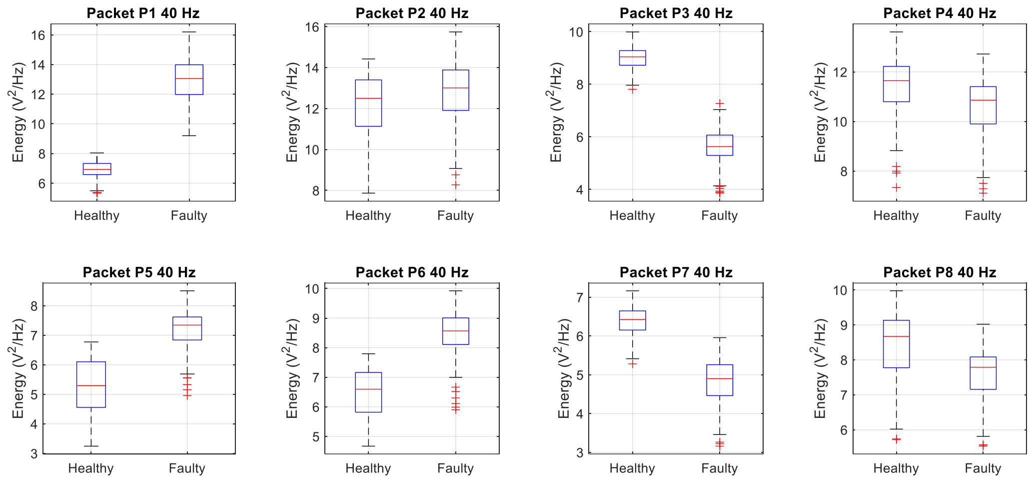

Figure 12. Boxplot representation of WPT packet energy distributions under healthy and looseness conditions at 40 Hz rotational speed. Boxplot elements are defined as in Figure 11.

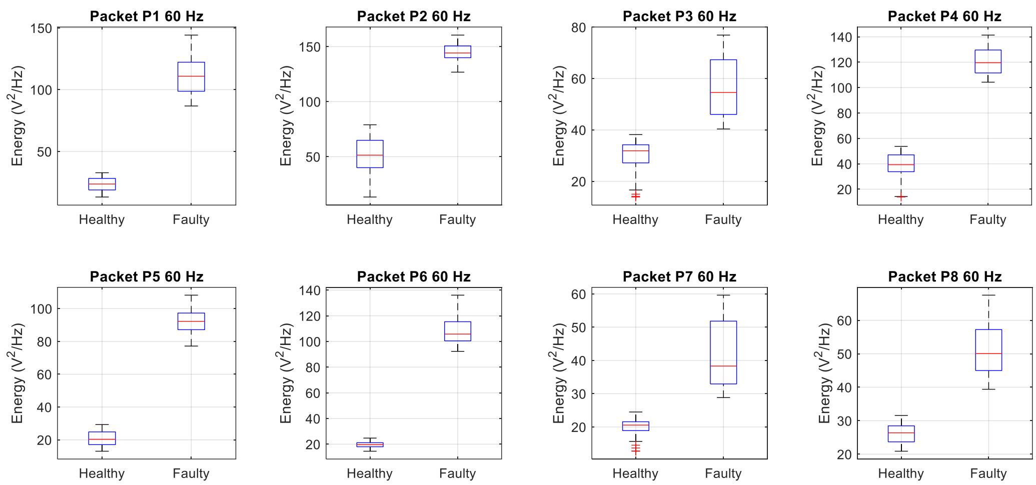

Figure 13. Boxplot representation of WPT packet energy distributions under healthy and looseness conditions at 60 Hz rotational speed. Boxplot elements are defined as in Figure 11.

The obtained boxplot distributions confirm the capability of the proposed NCA-based methodology to identify diagnostically informative WPT frequency regions associated with mechanical looseness.

3.5. Supplementary Level-4 WPT Refinement at 60 Hz

To further investigate the frequency localization of the looseness-related vibration components, an additional level-4 WPT decomposition was performed using the optimal mother wavelet identified under the 60 Hz operating condition.

While the level-3 decomposition enabled global identification of the most discriminative WPT regions, the higher-resolution analysis provided improved spectral localization of the fault-related vibration components.

The obtained NCA relevance map (Figure 14) revealed that the discriminative capability was primarily concentrated in packets P10 and P12, corresponding approximately to the frequency bands 2625–2812.5 Hz and 2437.5–2625 Hz, respectively.

The obtained results are consistent with the level-3 decomposition, in which packet P6 (2250–2625 Hz) exhibited the highest discriminative contribution. In the higher-resolution level-4 decomposition, packet P12 (2437.5–2625 Hz), corresponding to a subband contained within the original P6 region, remained highly relevant according to the NCA analysis.

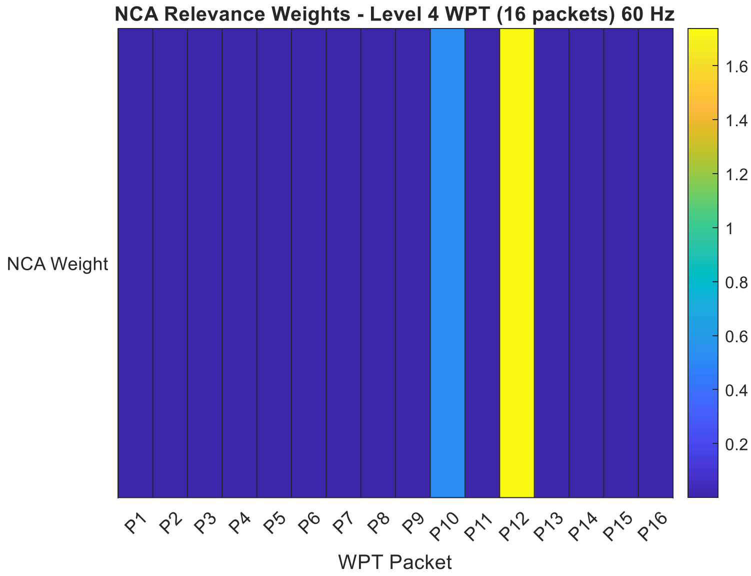

Figure 14. NCA relevance weights for a decomposition level of 4 at 60 Hz.

This behavior suggests that the level-3 decomposition successfully identified the global fault-sensitive frequency region, while the finer level-4 decomposition enabled improved localization of the discriminative vibration components associated with mechanical looseness.

Additionally, the comparison between the average WPT packet energies under healthy and looseness conditions revealed that the packets exhibiting the largest energy variations were not necessarily the most discriminative ones according to the NCA relevance analysis (Figure 15).

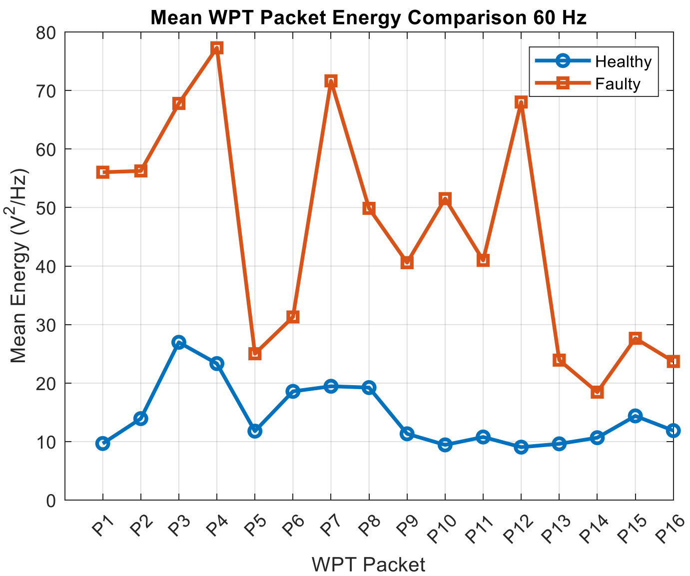

Figure 15. Mean WPT energy comparison at 60 Hz and a decomposition level of 4.

This observation highlights that diagnostic performance depends not only on the magnitude of the energy variation, but also on the statistical consistency and separability of the extracted features between operating conditions. Consequently, the proposed supervised relevance analysis methodology provides improved interpretability by identifying the WPT frequency regions that maximize fault separability rather than simply maximizing signal energy.

Although higher WPT decomposition levels provide finer frequency resolution, they also increase the number of packet-energy features and may reduce interpretability by fragmenting the vibration energy distribution into a larger feature space. For this reason, level-3 decomposition was selected as the baseline configuration for the comparative analysis performed in this study, since it provides eight WPT packets and offers a suitable compromise between frequency resolution, feature dimensionality, computational simplicity, and physical interpretability. The level-4 decomposition was therefore not intended to replace the level-3 analysis or to define a universally optimal decomposition level, but rather to act as a supplementary refinement step for further investigating specific frequency regions when the level-3 analysis showed concentrated fault-related relevance.

3.6. Overall Discussion

The obtained results demonstrate that the proposed methodology is capable of characterizing mechanical looseness through WPT-based vibration analysis and supervised feature relevance evaluation under varying operating conditions. Previous WPT-based studies have shown the usefulness of wavelet packet energy features for rotating machinery fault diagnosis [18,22–24]. However, in many cases, WPT is mainly used as a feature extraction tool, while the diagnostic interpretation relies on classification accuracy, empirical energy comparison, or visual analysis of time–frequency representations.

The main contribution of the present work lies in the supervised interpretability of the WPT energy representation. The proposed NCA-based methodology quantifies the discriminative relevance of each WPT packet, allowing objective mother wavelet comparison and identification of fault-sensitive frequency regions under different rotational speeds. NCA was selected because it assigns relevance weights directly to the original packet-energy features, preserving packet-level interpretability.

The observed speed-dependent changes in packet relevance can be physically related to the nonlinear nature of mechanical looseness. The presence of clearance produces intermittent contact and impact-like excitation, whose frequency and intensity vary with rotational speed. Therefore, looseness-related information is not expected to remain concentrated in the same frequency band under all operating conditions.

The results also showed that the WPT packets with the highest energy variations were not necessarily the most discriminative ones according to NCA. This confirms that diagnostic relevance depends not only on energy magnitude, but also on the consistency and separability of the extracted features between healthy and looseness conditions. The additional level-4 WPT analysis at 60 Hz provided improved localization of fault-sensitive high-frequency subbands, supporting the interpretation of speed-dependent energy redistribution.

Although the proposed approach shows potential for interpretable vibration-based condition monitoring, the experiments were conducted under controlled laboratory conditions using a single looseness severity and a limited set of rotational speeds. Future work should consider additional fault severities, variable loading conditions, combined defects, full-scale systems, and comparison with other feature selection or dimensionality reduction techniques.

4. Conclusions

This work presented a vibration-based methodology for mechanical looseness diagnosis in rotating shafts using Wavelet Packet Transform (WPT) energy analysis and supervised feature relevance evaluation through Neighborhood Component Analysis (NCA). The main scientific contribution of the study lies in the integration of WPT packet-energy features with supervised NCA-based relevance analysis, enabling not only fault-sensitive feature extraction but also interpretable identification of the WPT packets that contribute most strongly to the separation between healthy and looseness conditions.

The obtained results demonstrated that rotational speed significantly influences the distribution of looseness-related vibration energy within the WPT domain and the localization of the most discriminative frequency regions. The proposed methodology additionally showed that the most energetic frequency bands are not necessarily the most informative ones for fault diagnosis.

A level-3 WPT decomposition was selected as the baseline configuration for the comparative analysis because it provided an appropriate balance between frequency resolution, feature dimensionality, computational simplicity, and interpretability. The additional level-4 WPT analysis was included only as a supplementary refinement step to improve the spectral localization of fault-sensitive subbands in selected cases, rather than as the general decomposition level adopted for the complete methodology.

Regarding mother wavelet selection, the results showed that the most suitable wavelet depends on the operating condition. In particular, coif1 provided the highest discriminative capability at 20 Hz, sym2 achieved the highest cumulative NCA relevance score at 40 Hz, and sym5 was the best-performing wavelet at 60 Hz. These findings confirm that mother wavelet selection should not be considered independent of rotational speed.

Overall, the proposed approach provides an interpretable framework for objective mother wavelet evaluation, fault-sensitive packet identification, and analysis of speed-dependent vibration energy redistribution in rotating machinery. Nevertheless, the present study was limited to controlled laboratory conditions, a single imposed looseness severity, and three rotational speeds without external load. Future work should extend the validation to lower clearance levels, single-interface looseness faults, variable loading conditions, combined defects, full-scale rotating systems, and comparison with alternative feature selection techniques.

Author Contributions: Conceptualization, M.Z. and M.J.G.; methodology, M.Z.; software, M.Z.; validation, M.Z., M.J.G. and C.C.; formal analysis, M.Z.; investigation, M.Z.; resources, M.Z. and M.J.G.; data curation, M.Z.; writing—original draft preparation, M.Z.; writing—review and editing, M.J.G. and C.C.; visualization, M.Z.; supervision, C.C.; project administration, C.C.; funding acquisition, C.C. All authors have read and agreed to the published version of the manuscript.

Funding: This research was funded by the Agencia Estatal de Investigación (AEI) and the Ministerio de Ciencia e Innovación MCIN/AEI/10.13039/501100011033, grant number PID2024-160821OB-I00 and by the Madrid Government (Comunidad de Madrid—Spain) under the Multiannual Agreement with UC3M (MEMRIAAP-CM-UC3M).

Data Availability Statement: The data supporting the findings of this study can be downloaded at https://doi.org/10.21950/C89CN8.

Conflicts of Interest: The authors declare no conflicts of interest. The funders had no role in the design of the study; in the collection, analyses, or interpretation of data; in the writing of the manuscript; or in the decision to publish the results.

Abbreviations

The following abbreviations are used in this manuscript:

NCA	Neighborhood Component Analysis
WPT	Wavelet Packet Transform
COIF	Coiflets
SYM	Symlets
DB	Daubechies
DWT	Discrete Wavelet Transform

References

1. Yan, R.; Shang, Z.; Xu, H.; Wen, J.; Zhao, Z.; Chen, X.; Gao, R.X. Wavelet Transform for Rotary Machine Fault Diagnosis:10 Years Revisited. *Mech. Syst. Signal Process.* **2023**, *200*, 110545. [CrossRef]
2. Jardine, A.K.S.; Lin, D.; Banjevic, D. A Review on Machinery Diagnostics and Prognostics Implementing Condition-Based Maintenance. *Mech. Syst. Signal Process.* **2006**, *20*, 1483–1510. [CrossRef]
3. Lei, Y.; Li, N.; Guo, L.; Li, N.; Yan, T.; Lin, J. Machinery Health Prognostics: A Systematic Review from Data Acquisition to RUL Prediction. *Mech. Syst. Signal Process.* **2018**, *104*, 799–834. [CrossRef]
4. Zhang, Q.; Su, N.; Qin, B.; Sun, G.; Jing, X.; Hu, S.; Cai, Y.; Zhou, L. Fault Diagnosis for Rotating Machinery Based on Dimensionless Indices: Current Status, Development, Technologies, and Future Directions. *Electronics* **2024**, *13*, 4931. [CrossRef]
5. Lee, J.; Bagheri, B.; Kao, H.-A. A Cyber-Physical Systems Architecture for Industry 4.0-Based Manufacturing Systems. *Manuf. Lett.* **2015**, *3*, 18–23. [CrossRef]
6. Carvalho, T.; Soares, F.; Vita, R.; Francisco, R.; Basto, J.; Alcalá, S. A Systematic Literature Review of Machine Learning Methods Applied to Predictive Maintenance. *Comput. Ind. Eng.* **2019**, *137*, 106024. [CrossRef]
7. Tang, S.; Yuan, S.; Zhu, Y. Deep Learning-Based Intelligent Fault Diagnosis Methods Toward Rotating Machinery. *IEEE Access* **2020**, *8*, 9335–9346. [CrossRef]
8. Wu, T.Y.; Chung, Y.L.; Liu, C.H. Looseness Diagnosis of Rotating Machinery via Vibration Analysis Through Hilbert–Huang Transform Approach. *J. Vib. Acoust.* **2010**, *132*, 031005. [CrossRef]
9. Wei, Y.; Li, Y.; Xu, M.; Huang, W. A Review of Early Fault Diagnosis Approaches and Their Applications in Rotating Machinery. *Entropy* **2019**, *21*, 409. [CrossRef] [PubMed]
10. Li, Y.; Long, T.; Luo, Z.; Wen, C.; Zhu, Z.; Jin, L.; Li, B. Numerical and Experimental Investigations on Dynamic Behaviors of a Bolted Joint Rotor System with Pedestal Looseness. *J. Sound Vib.* **2024**, *571*, 118036. [CrossRef]
11. Zhou, P.; Chen, S.; He, Q.; Wang, D.; Peng, Z. Rotating Machinery Fault-Induced Vibration Signal Modulation Effects: A Review with Mechanisms, Extraction Methods and Applications for Diagnosis. *Mech. Syst. Signal Process.* **2023**, *200*, 110489. [CrossRef]
12. Zhou, P.; Peng, Z.; Chen, S.; Tian, Z.; Zuo, M.J. Sinusoidal FM Patterns of Fault-Related Vibration Signals for Planetary Gearbox Fault Detection under Non-Stationary Conditions. *Mech. Syst. Signal Process.* **2021**, *155*, 107623. [CrossRef]
13. Weak Fault Feature Extraction of the Rotating Machinery Using Flexible Analytic Wavelet Transform and Nonlinear Quantum Permutation Entropy. *Comput. Mater. Contin.* **2024**, *79*, 4513–4531. [CrossRef]
14. Kulevome, D.K.B.; Qiu, M.; Cao, F.; Opoku-Mensah, E. Evaluation of Time-Frequency Representations for Deep Learning-Based Rotating Machinery Fault Diagnosis. *Int. J. Eng. Technol. Innov.* **2025**, *15*, 314–331. [CrossRef]
15. Liang, R.; Ran, W.; Chen, Y.; Zhu, R. Fault Diagnosis Method for Rotating Machinery Based on Multi-Scale Features. *Chin. J. Mech. Eng.* **2023**, *36*, 141. [CrossRef]
16. Cichoń, A.; Berger, P.; Wotzka, D. Selecting Mother Wavelet for Wavelet Analysis of On-Load Tap Changer Acoustic Emission. *Acta Phys. Pol. A* **2015**, *128*, 310–315. [CrossRef]
17. Gao, L.; Wang, H.; Zhou, J.; Zhou, X. Selection of Optimal Mother Wavelet for Acoustic Emission Signal Processing of Gas Pipeline Leakage. In *Proceedings of the TEPEN 2022*; Zhang, H., Ji, Y., Liu, T., Sun, X., Ball, A.D., Eds.; Springer Nature: Cham, Switzerland, 2023; pp. 294–305.
18. Zamorano, M.; Gómez Garcia, M.J.; Castejón, C. Selection of a Mother Wavelet as Identification Pattern for the Detection of Cracks in Shafts. *J. Vib. Control* **2022**, *28*, 3152–3161. [CrossRef]
19. Zamorano, M.; Gómez, M.J.; Castejón, C. Optimal Selection of the Mother Wavelet in WPT Analysis and Its Influence in Cracked Railway Axles Detection. *Machines* **2023**, *11*, 493. [CrossRef]
20. Zamorano, M.; Gómez, M.J.; Castejon, C. An Analysis of the WPT Function for Pattern Optimization to Detect Defects in Bearings. *Machines* **2024**, *12*, 207. [CrossRef]
21. Zamorano, M.; Gómez, M.J.; Castejon, C.; Carboni, M. Analysis of Acoustic Emission Waveforms by Wavelet Packet Transform for the Detection of Crack Initiation Due to Fretting Fatigue in Solid Railway Axles. *Appl. Sci.* **2025**, *15*, 8435. [CrossRef]
22. Rafiee, J.; Tse, P.W.; Harifi, A.; Sadeghi, M.H. A Novel Technique for Selecting Mother Wavelet Function Using an Intelli Gent Fault Diagnosis System. *Expert Syst. Appl.* **2009**, *36*, 4862–4875. [CrossRef]
23. Wai Keng, N.; Leong, M.; Hee, L.; Abdelrhman, A. Wavelet Analysis: Mother Wavelet Selection Methods. *Appl. Mech. Mater.* **2013**, *393*, 953–958. [CrossRef]
24. Tran, H.; Noori, M.; Altabey, W.; Wu, X. Fault Diagnosis of Rotating Machinery Using Wavelet-Based Feature Extraction and Support Vector Machine Classifier. *High Speed Mach.* **2017**, *3*, 23–41. [CrossRef]
25. Maliuk, A.S.; Ahmad, Z.; Kim, J.-M. A Technique for Bearing Fault Diagnosis Using Novel Wavelet Packet Transform-Based Signal Representation and Informative Factor LDA. *Machines* **2023**, *11*, 1080. [CrossRef]
26. Gómez, M.J.; Castejón, C.; Corral, E.; García-Prada, J.C. Railway Axle Condition Monitoring Technique Based on Wavelet Packet Transform Features and Support Vector Machines. *Sensors* **2020**, *20*, 3575. [CrossRef] [PubMed]

27. Kumar, R.; Anand, R.S. Bearing Fault Diagnosis Using Multiple Feature Selection Algorithms with SVM. *Prog. Artif. Intell.* **2024**, *13*, 119–133. [CrossRef]
28. Bezerra, F.E.; de Oliveira Neto, G.C.; Cervi, G.M.; Francesconi Mazetto, R.; de Faria, A.M.; Vido, M.; Lima, G.A.; de Araújo, S.A.; Sampaio, M.; Amorim, M. Impacts of Feature Selection on Predicting Machine Failures by Machine Learning Algorithms. *Appl. Sci.* **2024**, *14*, 3337. [CrossRef]
29. MFS—Lite. Available online: https://spectraquest.com/machinery-fault-simulator-lite/ (accessed on 30 June 2026).
30. Jensen, A.; la Cour-Harbo, A. *Ripples in Mathematics*; Springer: Berlin/Heidelberg, Germany, 2001; ISBN 978-3-540-41662-3.
31. Goldberger, J.; Hinton, G.E.; Roweis, S.; Salakhutdinov, R.R. Neighbourhood Components Analysis. In *Proceedings of the Advances in Neural Information Processing Systems*; MIT Press: Cambridge, MA, USA, 2004; Volume 17.

https://doi.org/10.3390/machines14070779